

1
2
3
4
5 Bovine Milk Fat Globule Epidermal Growth Factor VIII
6 Activates PI3K/Akt Signaling Pathway and Attenuates Sarcopenia
7 in Rat Model Induced by D-galactose

8
9 He Li^{ab}, Rongchun Wang^b, Lifeng Wang^c, Lin Li^b, Ying Ma^{b*}, Shaobo Zhou^{bd}

10
11 ^aCollege of Health Sciences, Jiangsu Normal University, Xuzhou 221116, Jiangsu, PR
12 China.

13 ^bSchool of Chemistry and Chemical Engineering, Harbin Institute of Technology,
14 Harbin 150090, Heilongjiang, PR China.

15 ^cFood Science College, Northeast Agriculture University, Harbin 150036, Heilongjiang,
16 PR China.

17 ^dSchool of Life Sciences, Institute of Biomedical and Environmental Science and
18 Technology, University of Bedfordshire, Luton, LU1 3JU, UK.

19 *Corresponding authors: Phone: +86 451 86282903, E-mail: maying@hit.edu.cn

20
21 **Abstract**

22 To develop a more effective and safer treatment for sarcopenia, this research
23 investigated the anti-sarcopenia mechanism of Milk Fat Globule Epidermal Growth
24 Factor VIII (MFG-E8) from the liver function and metabolism in sarcopenic model rat.
25 After 4 weeks nutritional intervention experiment, MFG-E8 can significantly increase
26 the gastrocnemius mass in rat. The mechanism of MFG-E8 in improving sarcopenia was
27 related to its promotional capacity to the activities of superoxide dismutase (SOD)

28 activity in serum, Glutamic-oxaloacetic transaminase (GOT) and glutamic-pyruvic
29 transaminase (GPT) in liver. Meanwhile, MFG-E8 could also down-regulate
30 obesity-related indicators, such as triglyceride (TG) and Non-esterified fatty acid
31 (NEFA). The analysis of liver and gastrocnemius histopathology found that MFG-E8
32 could reduce the accumulation of fatty vesicles, improve liver function, thereby
33 alleviating gastrocnemius tissue inflammation. *In vitro* experiments, myoblasts obtained
34 from gastrocnemius tissue showed that MFG-E8 could reduce mitochondrial autophagy
35 and inhibit cell apoptosis. In addition, MFG-E8 could up-regulate the phosphorylation
36 level of PI3K *via* activating PI3K/Akt signaling pathway in gastrocnemius tissue, and
37 promote the formation of muscle fibers, thereby increasing muscle mass. Moreover,
38 MFG-E8 could also promote the formation of neuromuscular junctions by up-regulating
39 the mRNA and protein expression of MusK in gastrocnemius.

40 **Keywords:** MFG-E8; Sarcopenic model rat; Myoblasts; PI3K/Akt signalling pathway.

41 **1 Introduction**

42 Sarcopenia is a kind of aging-related degenerative diseases that occurs mainly in
43 the elderly populations. It is caused by imbalance of skeletal muscle protein anabolism
44 and catabolism, and also associated with metabolic chronic diseases, such as diabetes
45 and obesity, which pose threats to physical performance and life expectancy(Viana et al.
46 2013). Traditional hormonal drugs for treating sarcopenia have significant effects.
47 However, many steroid hormones drugs, for example, glucocorticoids, testosterone and
48 nandrolone, are poorly nutrient absorption and digestion, as well as a vicious circle,
49 which poses great risks to human health(Sakuma et al. 2017; Sakuma and Yamaguchi
50 2018). Resistance exercise is an effective way to increase muscle mass, loss weight, and
51 cardiometabolic health. It can enhance the activity of mitochondria and myoblasts
52 activity, but resistance exercise is dangerous for some elderly people(Elena et al. 2015;
53 Joe 2019). Therefore, new safer and more effective anti-sarcopenia nutrients are needed.
54 Currently, natural products, such as bioactive food components, have emerged as new
55 therapies that can overcome incidental risk of drugs(Sakuma and Yamaguchi 2018;
56 Yuan et al. 2018). Traditional food-borne nutrients, such as polyphenols, proteins,

57 bioactive peptides, are regarded as alternative methods in preventing and treating
58 sarcopenia.

59 Milk is the main source of nutrition in newborn mammals, milk fat globule
60 membrane (MFGM) is a mixture of primarily membrane proteins, phospholipid and
61 sphingomyelin(Nguyen et al. 2016). MFGM has attracted widespread attention in
62 anti-sarcopenia due to its potential nutritional value, *eg.* clinical trials in frail women
63 and healthy adults demonstrated that resistance exercise combined with dietary
64 supplementation and MFGM can reverse the deficits in skeletal muscle protein
65 metabolism imbalance and improve muscle mass and function.

66 Milk fat globule epidermal growth factor VIII (MFG-E8), a cysteine rich secretory
67 glycoprotein distributed in various tissues in mice and other mammalian species, has
68 been broadly used as Food functional factors and drugs for a long time(Aziz et al. 2017;
69 Cheyuo Cletus et al. 2019). MFG-E8 contains two N-terminal epidermal growth
70 factor-like domains (EGF domains), and C-terminal discoidin domains similar to the
71 blood coagulation factor-V/VIII (C₁ and C₂ domains)(Aziz et al. 2017; Cheyuo Cletus et
72 al. 2019). EGF₂ contains an Arg-Gly-Asp sequence and binds to integrins $\alpha v\beta 3$ and
73 $\alpha v\beta 5$, besides, C₂ domain has high affinity for membranes that contains
74 phosphatidylserine. The functions of MFG-E8 mainly focused on angiogenesis,
75 phagocytosis of apoptotic cells and cell matrix adhesion. The important health benefits
76 of MFG-E8 include suppressing autoimmune diseases, anti-tumor, suppressing
77 Alzheimer's disease, promoting angiogenesis and repairing intestinal function(Cheyuo
78 Cletus et al. 2019; Aziz et al. 2017). We have previously demonstrated *in vitro* C₂C₁₂
79 cells that MFG-E8 could promote cell proliferation and differentiation(He et al. 2017;
80 Li et al. 2017). Based on the results of cell differential proteomics, we clarified that
81 MFG-E8 promoting cell proliferation is related to 60S ribosomal protein L29, Hsp 40,
82 integrin α -V, serine/threonine protein phosphatase 2A and insulin degrading enzyme
83 expression, mediating PI3K, MAPK, AMPK and Oxidative phosphorylation signaling
84 pathways cascade, and PI3K plays a major role(Li et al. 2019). *In vitro* experiment
85 preliminarily demonstrated the possible benefits of MFG-E8 on sarcopenia(Li et al.

86 2018). However, to the best of our knowledge, the research of MFG-E8 on sarcopenia
87 has focused on the *in vitro* myoblasts model, so far, there are no related reports about
88 MFG-E8 *in vivo*(Li et al. 2017; Li et al. 2018).

89 Organs involved in the development of sarcopenia mainly include the liver, kidney,
90 skeletal muscle, brain and adipose tissue(Ponziani and Gasbarrini 2018; Sun et al.
91 2018).The liver, which is the primary organ for lipid and carbohydrate
92 metabolism(Qi-chen et al. 2019). Skeletal muscle and liver tissue are the primary site of
93 insulin-mediated glucose uptake(Manning and Toker 2017). Insulin-like growth factor
94 (IGF-I) regulates the proliferation and differentiation of cells with insulin-like
95 metabolism and nutrition, and is closely related to animal muscle growth and
96 development. PI3K/AKT pathway play a central role in the molecular mechanisms,
97 which regulate cellular energy metabolism and glucose metabolism(Zecic and
98 Braeckman 2020). Mitochondrial oxidative capacity was significant reduced in ageing
99 liver, which may act as an important contributor to the ageing process(Rygiel et al. 2017;
100 Joe 2019). Akt, known as protein kinase B, is a serine/threonine kinase, operates
101 downstream of PI3K, and has a key responsibility in regulation of energy metabolism at
102 both organismal and cellular levels(Qi-chen et al. 2019; Li et al. 2018). In addition,
103 IGF-I can regulate the differentiation of myoblasts by inducing the expression of key
104 factors such as MyoD, MEF2 and p21. The biological activity of IGF-I is regulated by
105 IGF-I receptors and IGF binding proteins, which play roles in promoting mitosis,
106 growth differentiation and insulin-like metabolic effects(Yu et al. 2015). Therefore, it
107 seems that insulin and IGF-I are in a tight relationship in terms of intracellular activities.
108 However, there are very limited data about the effect of MFG-E8 on IGF-I in
109 age-related sarcopenia subjects.

110 Aging is manifested as the decline of self-functions, decreased physical strength,
111 stress ability and energy metabolism accompanied by the occurrence of various
112 aging-related diseases(Zhou et al. 2016; Haifeng et al. 2005). Excessive injection of
113 D-gal can induce toxic and side effects on the body, mainly involve mitochondrial
114 dysfunction, generation of a large number of free radicals and lipid peroxidation,

115 accelerate the aging process of rats, and cause abnormal metabolic function of important
116 organs such as heart, liver and kidney. This impair syndrome exhibited senile
117 degenerative changes, and ultimately lead to varying degrees of damage and atrophy of
118 skeletal muscle fibers, highly similar to the clinical symptoms of sarcopenia. The rat
119 model of sarcopenia constructed by D-gal is reversible, and can be relieved and treated
120 through drug and nutritional intervention (Zhang et al. 2018; Sakuma and Yamaguchi
121 2018). Because of its small damage to the body and high survival rate, it can simulate
122 the sarcopenia caused by natural aging more accurately, so it is widely used in the
123 screening of senile sarcopenia drugs (Fan et al. 2017; Liao et al. 2014).

124 In this study, a sarcopenic model rat induced by injection of D-gal was established
125 to evaluate the repair and regeneration effects of MFG-E8. The effects of MFG-E8 on
126 liver and gastrocnemius dysfunction and histological lesion caused by sarcopenia were
127 carried out. Furthermore, considering the important role of the PI3K/Akt pathways in
128 metabolism, the effects of MFG-E8 on the activation of the PI3K/Akt pathways were
129 also investigated.

130 **2. Materials and methods**

131 The MFGM protein was separated from cow's milk (Harbin, Heilongjiang, China)
132 by an electric cream separator, MFG-E8 from the MFGM was prepared and separated
133 based on the cellulose DE-52 ion exchange chromatography treatment(He et al. 2017).
134 Sprague Dawley (SD) rats were purchased from the animal facility of the Second
135 Affiliated Hospital of Harbin Medical University (Harbin, Heilongjiang, China),
136 permission number: SCXK 2013-001.

137 **2.1 Experimental design**

138 **2.1.1 Animal model**

139 Sarcopenic model rats were carried out by following the literature procedure
140 (Zhang et al. 2018; Sun et al. 2018). 200 mg/kg D-galactose (D-gal) was administered
141 daily for 6 weeks through subcutaneous injection, control group was subcutaneous
142 injection same volume of 0.01 mol/L Phosphate buffered saline (PBS). Each rat was
143 kept in an isolated cage with free access to food and water (Table 1).

144 **2.1.2 Nutrition intervened**

145 Rats were randomly assigned to 3 groups (Table 1), MFGM or MFG-E8 was
146 administrated orally daily for 4 weeks days after 6 weeks of D-gal injection, asodium
147 pentobarbital anesthesia, while the rests were sacrificed by cervical dislocation, and the
148 blood, organs and tissues were taken out for biochemical assays. All surgeries were
149 performed under sodium pentobarbital anesthesia, and all the efforts were made to
150 minimize suffering. The body weight of the rats was measured weekly. All animal
151 protocols were approved by the animal ethics committee of Harbin Institute of
152 Technology, School of Life Science and Technology.

153 **2.2 Physiological and biochemical analysis**

154 **2.2.1 Tissue collection**

155 In the end of the expriments, the muscle weight (gastrocnemius and soleus), fat
156 tissue weight (epididymal and perienal) and tissue weight (liver, spleen and kidney)
157 were measured and harvested. Liver and gastrocnemius tissues were rapidly placed in
158 10% formaldehyde solution fixative as a biopsy for microscopy assessment.

159 **2.2.2 Biochemical analysiy**

160 Blood was collected from anesthetized rat heart under non-fasted conditions via
161 chloral hydrate vein. Plasma glucose, triglyceride (TG) and Non-esterified fatty acid
162 (NEFA) contents were measured with glucose, TG and NEFA testing kit (Lengton
163 Biosciencei, Shagnhai, China). The enzymatic activities of superoxide dismutase (SOD)
164 and the levels of Malondialdehyde (MDA) were measured with SOD and MDA testing
165 kits (Nanjing Jiancheng Bioengineering Institute, China) according to the
166 manufacturer's instructions. Insulin like growth factor 1 (IGF-1) was measured with a
167 rat IGF-1 Immunoassay kit (Lengton Biosciencei, Shagnhai, China).
168 Glutamic-oxaloacetic transaminase (GOT) and glutamic-pyruvic transaminase (GPT)
169 activity in liver were measured with GOT and GTP assay kits (Nanjing Jiancheng
170 Bioengineering Institute, China).

171 **2.3 Histological analysis**

172 Histopathological determine was performed by a pathologist at the hospital of

173 Harbin Institute of Technology. The gastrocnemius and liver samples were pre-fixed in
174 10% formaldehyde solution and washed with PBS buffer. The muscle samples were
175 vertically embedded in paraplast. Block prepared, frozen and cut muscle fragments into
176 5 μm thick sections. These sections were well-mounted on pre-silanated slides and dried
177 at 60 °C for 1 h, followed by dewaxing, hydration and staining with hematoxylin–eosin
178 (HE) (Pandey et al. 2014). These stained slides were dehydrated and mounted in
179 Permount. For the quantification of nuclei and muscle fibers and area measurement of
180 these fibers were magnified from 10 to 100x.

181 **2.4 The *In vitro* Assessment of MFG-E8 on myoblasts of gastrocnemius**

182 **2.4.1 Isolation and identification of myoblast**

183 The myoblasts were isolated according to Alessandra et al.'s (Alessandra Sacco
184 2008) with a slight modification. The large hind limb gastrocnemius of rats was isolated,
185 then non-muscle tissues were removed under a section microscope. The gastrocnemius
186 was subjected to enzymatic dissociation with 0.2% collagenase Type II (Solarbio, China)
187 for 60 min, then with 0.04 U/mL dispase II (Solarbio, China) for 45 min. The cell
188 suspension was filtered through a cell strainer.

189 Evaluation of myoblast proliferation and differentiation ability was according to
190 our previous research methods (Li et al. 2017). Myoblasts were grown in DMEM with
191 10% (v/v) FBS, 100 U mL⁻¹ penicillin, and 100 mg mL⁻¹ of streptomycin (Invitrogen) in
192 a humidified incubator containing 5% CO₂ at 37°C. The myoblasts were fused into
193 myotubes at 50% confluence by shifting the growth medium to a differentiation medium
194 consisting of DMEM supplemented with 2% horse serum. The morphological changes
195 of myoblasts were observed by light microscope.

196 **2.4.2 Effect of MFG-E8 on Cell cycle**

197 Cell cycle experiments were carried out on a BD FACS scan flow cytometer
198 (Bio-Rad) and Cell-Quest software (BD Biosciences), which describe in our previous
199 research (He et al. 2017).

200 **2.4.3 Effect of MFG-E8 on mitochondria**

201 Myoblasts were fixed with 4% glutaraldehyde at 4 °C for 12 hours, which were

202 collected by centrifugation. The cell pellets were fixed in 2.5% glutaraldehyde for 2 h
203 and with 1% osmium tetroxide for 2 h, then dehydrated in ascending ethanol serial
204 washes and embedded in Epon 812. Serial ultrathin sections were characterized by
205 transmission electron microscope (TEM, Zeiss 900, Germany).

206 **2.5.4 Effects of the MFG-E8 on the myoblasts proliferation and morphology**

207 Myoblasts were incubated with 1 mL of staining buffer, 5 mL of Hoechst 33342
208 (excitation 360 nm/emission 465 nm) buffer and 5 ml of PI staining (excitation 488 nm/
209 emission 620 nm) buffer for 20~30 min, then myoblasts were observed by confocal
210 laser scanning microscope (CLSM, Leica, Germany).

211 **2.5 qRT-PCR**

212 Total RNA in gastrocnemius was extracted using a RNeasy pure animal tissue kit
213 (Qiagen Biotech, Beijing). cDNA was synthesized using 3 mg of RNA with a
214 PrimeScript II 1st Strand cDNA Synthesis Kit (Takara, Ishiyama, Japan) according to
215 the manufacturer's instructions. The assay was carried out on an CFX96 Real-Time
216 PCR system (Bio-Rad Laboratories, USA) with iTaq™ Universal SYBR Green
217 Supermix (BIO-RAD, CA, USA). The qRT-PCR conditions were as follows: 95 °C for
218 5 s, followed by 40 cycles of 95°C for 10 s, and 60 °C for 30 s. Relative expression was
219 first quantified using a standard curve and $2^{-\Delta\Delta CT}$ formula, and normalised to GAPDH.
220 The primers used in this study were shown in Table 2.

221 **2.6 Western blot**

222 The method was based on our previous research(Li et al. 2018), total protein in
223 gastrocnemius was extracted by RIPA buffer with 10 mM PMSF, then the concentration
224 of protein was determined by BCA protein assay kit (Solarbio, China), and 10 mg
225 protein was electrophoresed in 10% SDS-PAGE gel. The proteins in gel were
226 transferred to nitrocellulose (NC) membrane carried out by Bio-rad electrotransfer
227 system. The NC membranes were incubated at 37 °C temperature for 1 h in blocking
228 buffer. Primary antibodies for each protein was incubated at 4 °C for 2 h. The
229 concentrations of the primary antibodies were anti-MusK (Bioss, China, 1:600),
230 anti-PI3K (Santa Cruz, USA, 1:500), anti-Akt (Santa Cruz, USA, 1:500), anti-p-Akt

231 (Santa Cruz, USA, 1:800), anti-mTOR (Santa Cruz, USA, 1:300) anti-p-mTOR (Santa
232 Cruz, USA, 1:500), anti-P70SK (Santa Cruz, USA, 1:800), anti-p-P70S6K (Santa Cruz,
233 USA, 1:800), anti-4E-BP (Santa Cruz, USA, 1:300), anti-p-4E-BP (Santa Cruz, USA,
234 1:400), and GAPDH (Santa Cruz, USA, 1:500). The NC membrane was washed by
235 TBST, following by incubation with secondary antibody (1:2000; Santa Cruz, USA) for
236 1 h at 37 °C. The NC membrane was washed by TBST and TBS, then incubated with
237 alkaline phosphatase. The protein band was detected by FluorChem Imaging Systems
238 (Alpha Innotech, Corp., San Leandro, CA, USA).

239 **2.7 Statistical analysis**

240 All experiments, except described somewhere else, were tested and analyzed in
241 triplicate. An analysis of variance (ANOVA) was identified to determine the significant
242 differences ($p < 0.05$) between means. The statistical analyses were done by using SPSS
243 19.0 (SPSS Science, USA).

244 **3 Results**

245 The MFG-E8 was extracted using an electric cream separator, and separated
246 according to cellulose DEAE-52 ion exchange chromatography method. Our previous
247 work has demonstrated that MFG-E8 can promote cell proliferation and differentiation
248 via the PI3K/Akt and ERK signal pathway in the *in vitro* C₂C₁₂ cells(Li et al. 2019). In
249 this study, we focused on the *in vivo* rat experiment to investigate the effect of MFG-E8
250 on age-related sarcopenia. The work flow was shown in Fig. 1.

251 **3.1 Construction and evaluation of sarcopenic model rats**

252 D-gal is a nutrient mainly obtained from lactose in milk, however, excessive intake
253 of D-gal can accelerate the aging process, accompanied by tissue and organ dysfunction,
254 resulting in metabolic abnormalities, which are the pathological characteristics of
255 aging-related sarcopenia(Zhang et al. 2018; Sun et al. 2018). Therefore, D-gal has been
256 widely used in exploring the targets of aging-related sarcopenia model and drug testing.
257 D-gal was injected into the subcutaneous of the rats for 6 weeks, based on the changes
258 of the rat's physical characteristics, physiology, biochemistry and organ coefficients to
259 evaluate whether the sarcopenic rats model was successfully constructed.

260 **3.1.1 Effects of D-gal on physiological and biochemical indices in rat**

261 To investigate the effect of D-gal on the basic physiological indexes of rats, we
262 recorded the data of initial weight, final weight gastrocnemius and soleus coefficient of
263 rats in 6 weeks (Table 3). Compared with normal group, the weight of rat increased
264 more slowly in D-gal group (Fig. 2A), after 6 weeks, the final weight of rats in D-gal
265 was also significantly lower than normal group (Table 3, $p<0.05$). The gastrocnemius
266 and soleus coefficients were calculated based on the final weight of the rats, results
267 showed that gastrocnemius and soleus coefficients of D-gal group were reduced by
268 11.3% and 12.5%, respectively ($p<0.05$), suggesting that D-gal induces impairment of
269 skeletal muscle mass in rat.

270 The tissue coefficients of kidney and liver were significantly lower in the D-gal
271 (Fig. 2B, $p<0.05$, versus normal group), and the kidney and liver were increased by
272 12.8 and 22.8%, respectively. However, the coefficient of spleen, epididymis adipose
273 and perirenal fat was no significantly different in D-gal ($p>0.05$, versus normal group).

274 SOD and MDA were used as indicators to evaluate the degree of aging, which can
275 regulated the dynamic imbalance among antioxidant capacity, free radical generation
276 and the degree of lipid peroxidation. SOD is the first enzymatic line of antioxidant and
277 an important enzyme in the antioxidant system, as shown in Fig. 2C, SOD activity in
278 the D-gal group was reduced by 22.6% ($p<0.05$, versus normal group). However, the
279 content of MDA in the D-gal group was increased by 38.6% ($p<0.05$, versus normal
280 group).

281 These results were similar to zhang et al.'s(Zhang et al. 2018) who have reported
282 that 200 mg/kg D-gal in the model group, which caused metabolic disorders and free
283 radical imbalance in the rat, accelerated the aging process of the rat, and resulted in a
284 decrease in the rate of increase in the gastrocnemius and soleus mass of the rats.

285 **3.1.2 gastrocnemius histopathology analysis**

286 The status of muscle fibers of gastrocnemius, affected by D-gal was further
287 observed using an inverted fluorescence microscope, and the results were shown in Fig.
288 2D. The muscle fibers of the gastrocnemius were seen to be arranged in fascicles

289 surrounded by connective tissue of normal appearance, with each fiber also surrounded
290 by connective tissue. Compared with normal group, the number of fibers and nuclei
291 decreased in the gastrocnemius of the D-gal treated rats ($p<0.05$), however, the diameter
292 of cells was increased and oedema of the cells was more serious in D-gal group. Besides,
293 there was significant difference in the total cross-sectional area, cells arrangement
294 irregularity, various forms of muscle fibers, and nuclei of the gastrocnemius between the
295 control and D-gal group (Fig. 2D). Combined with the results of physiological and
296 biochemical indicators, these results revealed that D-gal of 200 mg/kg could lead to
297 soleus and gastrocnemius injury, and the aging-related sarcopenic model rat was
298 successfully constructed by D-gal.

299 **3.2 MFG-E8 improved gastrocnemius and soleus in sarcopenia rats**

300 After MFGM or MFG-E8 treatment for 4 weeks, the average food intake of
301 sarcopenic model rat fed the normal diet (as control group) was not significantly
302 different from that of rats fed with MFGM and MFG-E8 (Table 4). Accordingly, the rat
303 body weight increased significantly after 4 weeks of MFGM or MFG-E8 treatment
304 ($p<0.05$, versus control group). The order of weight was as follows: MFG-E8
305 ($474.33\pm 18.43\text{g}$) > MFGM ($464.00\pm 12.46\text{g}$) > Control ($455.67\pm 10.34\text{g}$). The
306 gastrocnemius and soleus coefficient was significantly lower than that in the MFGM
307 (increased by 6.2% and 10.3%, respectively) or MFG-E8 (increased by 22.1% and
308 44.6%, respectively) group ($p<0.05$, versus control group); the gastrocnemius and
309 soleus coefficient was increased 28.8% and 10.7%, respectively ($p<0.05$, versus MFGM
310 group). The order of gastrocnemius coefficient was as follows: MFG-E8
311 (0.083 ± 0.002) > MFGM (0.075 ± 0.005) > Control (0.068 ± 0.008).

312 **3.3 Effect of MFG-E8 on tissue weights.**

313 The results of physiological indices demonstrated that the tissue coefficients of
314 kidney and liver were significantly higher in the MFGM and MFG-E8 group (Fig. 3A,
315 $p<0.05$, versus control group), and the kidney and liver were increased by 11.9% and
316 6.0%, respectively ($p<0.05$, versus MFGM group). In contrast, the epididymis adipose
317 and perirenal fat tissues mass were lower in MFGM and MFG-E8 group, but the

318 coefficient of epididymisadipose, perirenal fat, spleen and testis was no significantly
319 difference ($p>0.05$, versus control group).

320 **3.4 MFG-E8 improved antioxidant activity, liver function and lipid profile**

321 IGFs stimulate responses in skeletal muscle that include effects on carbohydrate
322 and lipid metabolism, protein turnover, growth, and differentiation. To assess more
323 characteristics directly related to aging, IGF-I cytokines in rat were measured by ELISA
324 (Fig. 3B). Compared with controls, IGF-I in MFGM or MFG-E8 group was increased
325 by 5.7 % and 48.6%, respectively (Fig. 3B, $p<0.05$).

326 The effects of MFG-E8 on the antioxidant activity were summarized in Fig. 3C,
327 the SOD activity in the MFGM or MFG-E8 group was increased by 13.6% and 33.6%,
328 while MDA content was reduced by 12.4% and 41.9%, respectively ($p<0.05$, versus
329 control group). It shows that MFGM, especially MFG-E8, could improve the
330 scavenging ability of superoxide anion free radicals in rats, reduce the accumulation of
331 harmful substances in the cells of rats, and delay the aging process.

332 Glutamic-oxaloacetic transaminase (GOT) and glutamic-pyruvic transaminase
333 (GPT) exist in the mitochondria and cytoplasm of all cells. The increase in the activity
334 of GOT and GPT correlates in general well with the extent and severity of cellular
335 damage, and is a basic procedure for diagnosing and monitoring hepatocellular diseases
336 or muscle damage. Liver function, as represented by GOT and GPT activities, improved
337 in model rat and this effect was significantly increased by MFG-E8 consumption (Fig.
338 3D).

339 In addition, MFG-E8 feeding decreased obesity-related metabolic parameters in rat,
340 including the epididymisadipose, perirenal fat, serum TG and serum NEFA (Fig. 3E,
341 epididymisadipose and perirenal fat coefficient: $p>0.05$, TG and NEFA: $p<0.05$, versus
342 control and MFGM group). We noticed that MFGM and MFG-E8 showed no effect on
343 the rat's food intake, but it can effectively increase body weight, gastrocnemius and
344 soleus coefficient and improve obesity-related metabolic parameters (Table 4, $p<0.05$,
345 versus control group).

346 **3.5 MFG-E8 ameliorated pathological changes of liver and gastrocnemius**

347 Histological examination of liver sections by staining with haematoxylin–eosin
348 revealed a loss of cellular integrity and an excessive fat accumulation in the liver of
349 control group, which exhibited more and large hepatic lipid droplets and more severe
350 steatosis compared with the MFGM and MFG-E8 treated groups. The hepatic lipid
351 droplets were disappeared almost completely, and hepatocytes were increased after
352 MFGM, especially MFG-E8 treatment (Fig. 4A). Hepatic morphology exhibited that
353 MFG-E8 treatment suppressed hepatic fatty acid accumulation and deposition, and
354 thereby preventing the formation of lipid droplets in hepatocytes. This trend is similar
355 with the effect of MFG-E8 administration on liver and plasma lipid profiles, which
356 suggest that MFG-E8 can down-regulate lipid accumulation in liver.

357 In comparison with control group, the spacing of muscle fiber became smaller and
358 dense, and cell nucleus was significantly increased in model rats treated by MFGM and
359 MFG-E8 (Fig. 4B); In addition, the rat also showed the direct evidence of muscle
360 atrophy in control group, eg: MFGM and MFG-E8 could effectively alleviate oedema of
361 the cells and muscle fiber atrophy. Compared with control, MFGM, especially for
362 MFG-E8 showed an effective way to alleviate muscle atrophy as a nutritional element.
363 Muscle atrophy or degenerative changes was significantly improved in the MFG-E8
364 group. These results indicated MFG-E8 could improve aging-related muscle atrophy.

365 **3.6 The *In vitro* Assessment of MFG-E8 on myoblast of sarcopenic rats**

366 **3.6.1 Isolation and Characterization of Myoblast**

367 The cell morphology and differentiation ability were observed through an inverted
368 microscope (Fig. 5). The cells isolated from the gastrocnemius of the three groups of
369 rats exhibited an elliptical/spindle shape (Fig. 5A) and had the ability to differentiate
370 into muscle fibers (Fig. 5B), and the MFG-E8 group had the strongest cell
371 differentiation ability ($p < 0.05$, versus control group). The results proved that the cells
372 isolated from the gastrocnemius tissue were myoblasts.

373 **3.6.2 Effects of MFG-E8 on the myoblast**

374 To determine the effect of MFG-E8 on myoblast, the changes of MFG-E8 treated

375 in cell cycle, cell activity, cell morphology and structure were analyzed. There was a
376 2.87% decrease in the G0/G1 population, and 0.54% and 12.77% decreases in S and
377 G2/M populations in myoblast treated with MFGM (Fig. 6A). Compared with the
378 control group, the G0/G1 and S population decreased by 11.90%, while the S and G2/M
379 population increased by 17.94% and 8.00% in cells treated with MFG-E8.

380 Mitochondrial dysfunction in skeletal muscle has been considered as a crucial step
381 in the development of metabolic diseases. Inherent or acquired mitochondrial disorders
382 can cause major disruption of cell survival and metabolic homeostasis (Joe 2019).
383 Further to investigate the effect of MFG-E8 on mitochondrial of myoblast was shown in
384 Fig. 6B. The mitochondria appeared to autophagy, vacuoles and formed unclear edges
385 in controls. Compared with control group, the mitochondrial number increased and
386 mitophagy was alleviated in the MFGM and MFG-E8 group.

387 The effect of MFG-E8 on myoblast morphology was further detected by CLSM
388 (Fig. 6C). The microscopic observation results showed that cell density significant
389 increased in MFG-E8 group, and the surface morphology of myoblasts showed no
390 significant change in MFGM and MFG-E8 group. However, the proportion of apoptotic
391 cells decreased (Fig. 6C). Combined with cell cycle, CLSM and TEM results, the cell
392 repairment and anti-apoptotic effect conducted by MFG-E8 may cause by the increase
393 of mitochondria.

394 Taken together, the measurement of gastrocnemius weight showed that
395 gastrocnemius coefficient leads to 15%-20% muscle loss in the sarcopenic model rats
396 (Table 3, $p < 0.05$, versus control group); while MFGM (~6.5%), especially for
397 MFG-E8-treated group, significantly reduced the loss of muscle mass (~44.63%) in
398 sarcopenic model rats (Table 4, $p < 0.05$, versus control group). Consistent with the *in*
399 *vitro* morphological data, the MFG-E8 could exert its protective effect against muscle
400 atrophy in rat muscle fibers as well.

401 **3.7 Effect of MFG-E8 on mRNA and protein expression levels**

402 The mRNA levels of MyoD, MyoG, Cyclin D1, IGF-I, Dok-7 and MusK were
403 determined by qRT-PCR (Fig. 7). the levels of Cyclin D1, MyoD and MyoG mRNA in

404 the MFGM group were increased by 15%, 88% and 63%, respectively, while the levels
405 of IGF-I and MusK mRNA in the MFGM group were significant increased by 25% and
406 21%, respectively (Fig. 8A, $p < 0.05$, versus control group). The levels of MyoG, Cyclin
407 D1, IGF-I and MusK in the MFG-E8 group were significantly increased by 65%, 39.2%,
408 41.7%, 14.9% and 78.1%, respectively, while the MyoD mRNA level was reduced by
409 44.6% (Fig. 8A, $p < .05$, versus MFGM group).

410 Muscle-specific tyrosine kinase (MusK) and Dok-7, both of which play essential
411 roles in synapse formation at the neuromuscular junction (NMJ), lack of MusK and
412 Dok-7 can lead to the failure of NMJ formation (Punga et al. 2015). Corresponding to
413 the results of qRT-PCR, MusK proteins were analysed further with *western blot* assay
414 (Fig. 7B). The expression of MusK in the MFG-E8 group up-regulated 39.4% over
415 control and MFGM. This result was similar to Haramizu (Haramizu et al. 2014a) who
416 has reported that MFGM, especially for resistance exercise combined with dietary
417 nutritional supplementation with MFGM, could improve muscle function deficits via
418 neuromuscular development in aging-related sarcopenia mouse.

419 **3.8 Effect of MFG-E8 on the activation of PI3K/AKT signaling pathway**

420 Mitochondria play crucial roles in energy metabolism, the PI3K/Akt signaling
421 pathway plays a crucial role in a variety of basic cell processes, including proliferation,
422 apoptosis, cell survival and metabolism (TF et al. 2003). To investigate the possible
423 effect of MFG-E8 activates PI3K/Akt signaling pathway, the expressions of PI3K
424 protein and phosphorylation levels were determined in gastrocnemius. Compared with
425 control group, MFGM did not significantly affect protein expression of PI3K, Akt and
426 mTOR (Fig. 8A-C, $p > 0.05$, versus control group) but could significantly up-regulated
427 the expression of phosphorylated PI3K, Akt and mTOR, especially MFG-E8 group
428 ($p < 0.05$). MFGM contains more than four hundred proteins (Ji et al. 2017), among them,
429 MFG-E8 is a high abundant protein in MFGM protein (~30%), indicating that MFG-E8
430 is a key functional factor in MFGM that could activate the PI3K signaling pathway.

431 MFG-E8 not only increase the total PI3K, AKT mTOR and P70S6K protein levels
432 but also increase the phosphorylated PI3K, AKT, mTOR and P70S6K protein levels

433 (Fig. 8A-D, $p < 0.05$, versus control), whereas the transcriptional activities of p-4E-BP
434 were decreased (Fig. 8E, $p < 0.05$, versus control). This result was similar to our previous
435 research *in vitro* cell experiment(Li et al. 2018), it can be speculated that MFG-E8 may
436 have a certain impact on the translation process of the protein, that is, there may be a
437 mechanism that promote protein synthesis and inhibit protein degradation. the
438 p-70S6K/p-70S6K and p-4E-BP/4E-BP levels in the MFG-E8 group were up-regulated
439 by 37.3% and down-regulated by 11.5%, respectively. The results indicated that
440 MFG-E8 could promote the proliferation, differentiation and myofibroblast formation of
441 myoblasts by activating the PI3K signaling pathway, thereby achieving the purpose of
442 repairing the damaged gastrocnemius.

443 **4. Discussion**

444 Sarcopenia is closely related to many metabolic diseases, such as obesity, abnormal
445 glucose metabolism or diabetes, hypertension and dyslipidemia(Angulo et al. 2016).
446 Although there is a clear classification of drugs for sarcopenia, side effects are still
447 serious during clinical use. So the choice of more effective and safer treatment for
448 sarcopenia has been become attractive. In recent years, more and more researches focus
449 on natural products that tried as novel therapeutic agents for sarcopenia, most of them
450 involved herbal plants extracts or foodborne plants, such as epigallocatechin gallate,
451 saponins flavonoids, curcumin, and ginsenosides, etc(Sakuma and Yamaguchi 2018).
452 Only a few studies have focused on the role of milk protein in preventing sarcopenia,
453 such as whey and MFGM(Minegishi et al. 2016). The branched-chain amino acids of
454 the hydrolysate of whey protein could promote the proliferation of myoblasts by
455 activating the IGF-I/PI3K/Akt signaling pathway(Jean et al. 2014). MFGM produced by
456 milk fat has an anti-sarcopenia effect caused by upregulating the expression of MusK
457 and Dok-7 in clinical trials(Haramizu et al. 2014b; Hari et al. 2015); MFG-E8 isolated
458 from milk exhibited more potential efficacy than MFGM in mitochondrial protection,
459 and proposed that it could regulate C₂C₁₂ cell proliferation by activating PI3K, MAPK,
460 Oxidative phosphorylation and AMPK signaling cascades.

461 MFGM has been used worldwide for many years as commercially available health

462 foods and has been considered beneficial to health. MFG-E8 is secreted from the
463 mammary epithelium during milk production as a high abundant protein in MFGM.
464 MFG-E8 also expressed in a wide range of organ tissues by a large variety of cells
465 including macrophages, fibroblasts, dendritic and epithelial cells(Li et al. 2017; Ji et al.
466 2017). In addition, a large number of literatures have reported the function, nutrition and
467 physiological characteristics of MFG-E8 in recent years. Based on the previous work, in
468 this paper, we for the first time investigated the anti-sarcopenia mechanism of MFG-E8
469 *in vivo*. The basic principles for establishing aging-related sarcopenia model based on
470 current research were as follows: As an inducer of aging *in vivo*, D-gal have been
471 widely used for exploring the targets of aging D-gal and drug testing(Zhang et al. 2018;
472 Sun et al. 2018). The aging rat induced by D-gal exhibited a dramatically
473 aging-associated decline in endurance capacity, oxygen consumption, and fat oxidation
474 associated with decreased fatty acid β -oxidation. Therefore, it could be concluded that
475 this was a suitable model that conforms to similar pathogenesis in humans, and can thus
476 be used to study the causes and pathogenesis of metabolic disorders involving
477 sarcopenia and to screen for potential use as treatment. In this study, the results of our
478 data in Section 3.1 showed gastrocnemius coefficient, kidney and liver coefficient, and
479 SOD/MDA in sarcopenic model rats decreased along with the daily treatment, and
480 inter-striated muscle cell edema and wax-like degeneration appeared, which meant the
481 sarcopenia model was successfully established(Liao et al. 2014; Zhang et al. 2018).

482 Aging process is precisely controlled by a giant signaling network that included
483 energy homeostasis, cellular metabolism and stress resistance(M; Nair K Sreekumaran;
484 Kahn C Ronald; 2019). Oxidative stress is a physiological and pathological reaction in
485 concert with increasing age, manifested as elevated free radicals leading to metabolic
486 disorders and inducing myoblast apoptosis, which can further cause the imbalance and
487 dysfunction of muscle protein(Zecic and Braeckman 2020). SOD and MDA are
488 important parameters to evaluate the levels of free radicals and oxidative stress(Wei et al.
489 2016). MDA is the secondary product of lipid peroxidation used as reactive aldehyde
490 that could make cross-linking between intramolecular and intermolecular and interact

491 with proteins to exert a toxic effect on the cells(Ruiz et al. 2012). SOD is also regarded
492 as the primary defense system against ROS and may reflect the ability of scavenging
493 free radicals(Wei et al. 2016; b et al. 2020). In present study, MFG-E8 could enhance
494 SOD activity and reduce MDA content, accelerate the scavenging of free radicals, and
495 improve the antioxidant capacity, SOD and MDA was negatively correlated. In addition,
496 Fatty acid metabolism is mainly characterized by elevated levels of NEFA, a predom
497 raised TG and low high density lipoprotein cholesterol levels, small dense low-density
498 lipoprotein cholesterol particles and raised apolipoprotein B values postprandial
499 hyperlipidaemia may also be present. Some emerging evidence also suggests that the
500 accumulation of lipids within skeletal muscle fibers may lead to metabolic disease, such
501 as insulin resistance(Janssen and Ross 2005). The mTOR is a conserved
502 serine-threonine kinase that regulates cell growth and metabolism in response to
503 nutrient signals. mTOR play a significant role both in “energy sensing” and in
504 regulation of energy production through profound effects on hepatic fatty acid
505 metabolism in rat(Joe 2019; Yamane et al. 2017). The levels of NEFA and the content of
506 TG in serum were decreased (Fig. 3E), in contrast, the liver coefficients, GTP and GOT
507 activity were increased, and the content of hepatic lipid droplets was reduced in
508 histopathological sections of liver (Fig. 3D). It suggested that MFG-E8 improve
509 aging-induced oxidative stress, fatty acid metabolism and promote the repair and
510 regeneration of gastrocnemius, which is related to the activity of intracellular
511 mitochondria. It is similar to Swiątecka who demonstrated that dairy proteins, eg:
512 MFGM, whey protein or casein have the potential to suppress postprandial lipaemia due
513 to their insulinotropic effects(Swiątecka et al. 2017; Qi-chen et al. 2019). Based on
514 these results, the repair and regeneration effect of MFG-E8 on sarcopenia is, at least
515 partially, attributed to the protection of the liver.

516 Apoptosis, oxidative stress, mitochondrial dysfunction and inflammation are
517 important factors in the occurrence of sarcopenia. Apoptotic cells and potentially toxic
518 substances are the result of aging-related neurodegenerative diseases and normal aging
519 processes. Effective removal of apoptotic substances is essential to protect surrounding

520 tissues from damage by proteins released by apoptotic cells(Cheyuo Cletus et al. 2019).
521 In the aging-related sarcopenia population, due to insufficient secretion of their own
522 growth factors and hormone levels, insufficient intracellular ATP energy supply result in
523 increased cytoplasmic Ca²⁺ concentration, finally leading to the number and activity of
524 muscle cells decrease, and even cause cell apoptosis(He et al. 2017; Wang et al. 2016).
525 Based on *in vitro* gastrocnemius myoblasts experimental results, MFG-E8 has no
526 significantly effect on the surface morphology of myoblasts. The structure of mitophagy
527 and vacuolar was reduced, and the number of cells in S phase and G2/M phase
528 increased, which promoted the synthesis of cell division-related enzymes and spindle
529 filament proteins, accelerated the process of cell mitosis to promote cell proliferation. In
530 addition, as the number of mitochondria increases, their activity, intracellular Ca²⁺ and
531 cyclic adenylyate content increases, which further enhance Akt phosphorylation(Rygiel et
532 al. 2017; Joe 2019). Activated Akt can negatively affect autophagy by regulating the
533 phosphorylation of mTOR, further promoting muscle protein synthesis and enhancing
534 muscle contraction(Jianbo et al. 2019). Therefore, MFGM, especially for MFG-E8
535 increased the number of myoblast of the aged rats *in vivo* and *in vitro*, promoted their
536 differentiation compared with controls, which could be the mechanisms that the skeletal
537 muscle weight increased, and accelerated the regeneration of injured skeletal muscles in
538 aged rats compared with controls.

539 IGF-I maintains the functions of skeletal muscle development mainly by: i)
540 promoting protein anabolism; ii) inhibiting protein catabolism. Besides, IGF-I can
541 regulate the differentiation of myoblasts by inducing the expression of key factors such
542 as MyoD, MEF2 and p21. IGF-I can also mediate the physiological role of growth
543 hormone (GH) in peripheral tissues. GH is secreted by pituitary gland and binds to GH
544 receptor to stimulate local tissue synthesis and secretion of IGF-I, however, excessive
545 IFG-I inhibits growth factor secretion, which limits the efficiency of IGF-I translation
546 initiation/translation extension and reduces the rate of gastrocnemius protein
547 synthesis(Webster et al. 2001; Yu et al. 2015). In this regard, MFG-E8 attenuates
548 aging-related sarcopenia by promoting the level of IGF-I in serum and IGF-I mRNA

549 expression in gastrocnemius, suggesting that MFG-E8 might attenuate dyslipidemia by
550 improving lipid metabolism in liver tissue.

551 The PI3K/Akt signaling pathway plays a crucial role in a variety of basic cell
552 processes, including proliferation, apoptosis, cell survival and metabolism(TF et al.
553 2003). The PI3K-related signaling pathway is not only related to the proliferation of
554 C₂C₁₂ cells, but also regulate the expression of myogenic regulatory factors: MyoD,
555 MyoG and MyHC, and participate in the regulation of the proliferation, differentiation
556 and fusion of muscle C₂C₁₂ cells to form multinucleated myotubes, which eventually
557 develop into mature muscle fibers(Li et al. 2017). Akt is a serine/threonine kinase,
558 operates downstream of PI3K, and plays a key role in the regulation of energy
559 metabolism at both organismal and cellular levels. Akt was also found to alter PI3K/Akt
560 signaling in the skeletal muscle of young men with low birth weight(Jensen et al. 2008).
561 mTOR is a downstream effector of Akt. Akt was phosphorylated on Thr308 in the
562 catalytic domain and Ser473 in the C-terminal domain by PDK1 and PDK2,
563 respectively, which were critical for Akt activation(He L et al. 2019; Li et al. 2018).
564 Phosphorylated Akt can improve the function of mTOR by phosphorylation at Ser2448,
565 which could up-regulate the expression of P70S6K phosphorylation and down-regulate
566 the expression of 4E-BP phosphorylation to regulate protein metabolism balance(Li et al.
567 2018). Based on these research, we investigated the mechanism of action of MFG-E8 on
568 the expression pattern of gastrocnemius in an *in vivo* rat model with qRT-PCR and
569 *western blot*. It was also observed that activated Akt phosphorylates the 2448 position
570 of mTOR, mTOR was activated, which regulates gastrocnemius protein synthesis and
571 degradation through two ways: (i) up-regulate the phosphorylated expression of
572 P70S6K protein to promote protein synthesis; (ii) down-regulate the phosphorylated
573 expression of 4E-BP1 to inhibit protein degradation.

574 The process of myogenic proliferation and differentiation is largely controlled by
575 the transcription factors of myogenic regulatory factor (MRF) family, such as MyoD,
576 MyoG and Myf5, which regulate the expression of several muscle-specific
577 genes(Conerly et al. 2016; Zammit and S. 2017). MyoD is a skeletal muscle-specific

578 protein that is able to induce myogenesis in a large variety of cell types, and considered
579 as a marker for terminal specification to the muscle lineage(Conerly et al. 2016). MyoG
580 not only can regulate its own expression, but also can interact with other transcription
581 factors of MRF, such as MyoD and Myf5, which is necessary for myoblast
582 differential and fusion *in vivo*(Zammit and S. 2017). MyoD activity has been shown
583 to correlate with the induction of the CDK inhibitor p21(Li et al. 2017). Our previous
584 results indicated that the PI3K/Akt-mediated signaling pathway can regulate the activity
585 of MyoD and MyoG by enhancing its transcriptional activity. Cyclin D1 is a key target
586 of proliferation signals, which could activate CDK4 by changing the G1 components.
587 Akt could induce cell proliferation by regulating its downstream cyclin D1, cyclin D2,
588 CDk 4 and p21 levels(Jianbo et al. 2019). The relevance of the AKT/GSK3 β /CyclinD1
589 pathway in the proliferation of hepatocellular carcinoma cells has also been
590 demonstrated by Xi, who showed that Akt expression is associated with a tendency for
591 increasing the expression of the hepatocellular carcinoma cells proliferation marker,
592 cyclin D1(Jianbo et al. 2019). In this research, MFG-E8 can accelerate the
593 differentiation and fusion process of myoblasts by up-regulating MyoG gene expression
594 in myoblasts of gastrocnemius tissue, which is consistent with the results of HE staining,
595 and these results were similar to our previous studies, therefore, MFG-E8 can
596 effectively promote the proliferation, differentiation and fusion of myoblasts, and
597 further promote the formation of gastrocnemius fibers.

598 In summary, *in vivo*, MFG-E8 treatment increased the gastrocnemius coefficient,
599 regenerated capacity of injured muscles, improved oxidative stress and fatty acid
600 metabolism compared with controls in sarcopenia rats via activating PI3K/Akt-signaling
601 pathway. *In vitro*, myoblast proliferation, differentiation, apoptosis and mitochondrial
602 autophagy were improved compared with controls in isolated myoblast from sarcopenia
603 rats. These results indicated that MFG-E8 has a beneficial effect on preventing
604 aging-related sarcopenia by activating the PI3K/Akt signaling pathway (Fig.9).

605 **5 Conclusion**

606 This study investigated the mechanism of MFG-E8 in improving sarcopenia *in vivo*

607 for the first time. MFG-E8 regulated oxidative stress and fatty acid metabolism level
608 through down-regulating the level of MDA, IGF-I, TG and NEFA in serum,
609 up-regulating the SOD activity and SOD/MDA. Inter-striated muscle cell edema and
610 wax-like degeneration were improved in gastrocnemius, and the fat content was reduced
611 in liver. *In vitro*, MFG-E8 alleviated apoptosis and mitochondrial autophagy of
612 myoblasts isolated from rats. MFG-E8 also up-regulated mRNA and protein expression
613 of IGF-I, MUSK, PI3K, Akt, mTOR and P70S6K, as well as down-regulated 4E-BP
614 protein expression in gastrocnemius. This research puts in new knowledge about the
615 potential mechanism of MFG-E8 in alleviating sarcopenia, which provides a new
616 evidence for the scientific and rational use for MFG-E8 in the improvement of
617 sarcopenia. Given these results, it can be affirmed that MFG-E8 could be a potential
618 anti-sarcopenia function factor and improve liver condition.

619 **Conflict of interest**

620 The authors declare no conflicts of interest

621 **Acknowledgments**

622 The author thanks the China Scholarship Council for a special scholarship award
623 [2018]3101.

624 **Reference**

- 625 Alessandra Sacco RD, Peggy Kraft, Stefan Vitorovic, Helen M Blau (2008)
626 Self-renewal and expansion of single transplanted muscle stem cells. *Nature*.
627 456, 502–506.
- 628 Angulo J, El Assar M & Rodríguez-Manas L (2016) Frailty and sarcopenia as the basis
629 for the phenotypic manifestation of chronic diseases in older adults. *Molecular*
630 *Aspects of Medicine*. 50, 1-32.
- 631 Aziz M, Hansen LW, Prince JM & Ping W (2017) Chapter 2 – Role of MFG-E8 in
632 Neonatal Inflammation. *Dairy in Human Health & Disease Across the Lifespan*,
633 21-30.

634 b LCa, b QJ, b H-lZa, b X-xD, a PG & b HJ (2020) The petrosal vein mutilation affects
635 the SOD activity, MDA levels and AQP4 level in cerebellum and brain stem in
636 rabbit. *Journal of Chemical Neuroanatomy*. 106, 101791-101797.

637 Cheyuo Cletus, Aziz Monowar & Ping W (2019) Neurogenesis in Neurodegenerative
638 Diseases: Role of MFG-E8. *Frontiers in neuroscience*. 13, 1-9.
639 <http://dx.doi.org/10.3389/fnins.2019.00569>.

640 Conerly M, Yao Z, Zhong JW, Groudine M & Tapscott S (2016) Distinct Activities of
641 Myf5 and MyoD Indicate Separate Roles in Skeletal Muscle Lineage
642 Specification and Differentiation. *Developmental Cell*. 36(4), 375-385.

643 Elena B, Deborah A, Emanuela P, Lucia P, Michele G, Francesco L, Giosuè A, Laura S,
644 Mauro DS & Vilberto S (2015) The Pleiotropic Effect of Physical Exercise on
645 Mitochondrial Dynamics in Aging Skeletal Muscle. *Oxidative Medicine &
646 Cellular Longevity*(4), 1-15. <http://dx.doi.org/10.1155/2015/917085>.

647 Fan J, Yang X, Li J, Shu Z, Dai J, Liu X, Li B, Jia S, Kou X & Yang Y (2017)
648 Spermidine coupled with exercise rescues skeletal muscle atrophy from
649 D-gal-induced aging rats through enhanced autophagy and reduced apoptosis via
650 AMPK-FOXO3a signal pathway. *Oncotarget*. 8(11), 17475-17490.

651 Haifeng, Qiujie & Song (2005) Behavioural study of the D-galactose induced aging
652 model in C57BL/6J mice. *Behavioural Brain Research*. 157(2), 245-251.

653 Haramizu S, Mori T, Yano M, Ota N, Hashizume K, Otsuka A, Hase T &
654 Shimotoyodome A (2014a) Habitual exercise plus dietary supplementation with
655 milk fat globule membrane improves muscle function deficits via neuromuscular
656 development in senescence-accelerated mice. *Springerplus*. 3(1), 1-17.

657 Haramizu S, Mori T, Yano M, Ota N, Hashizume K & Shimotoyodome A (2014b)
658 Habitual exercise plus dietary supplementation with milk fat globule membrane
659 improves muscle function deficits via neuromuscular development in
660 senescence-accelerated mice. *Springerplus*. 3(1), 1-17.

661 Hari S, Ochiai R, Shioya Y & Katsuragi Y (2015) Safety evaluation of the consumption
662 of high dose milk fat globule membrane in healthy adults: a double-blind,

663 randomized controlled trial with parallel group design. Journal of the
664 Agricultural Chemical Society of Japan. 79(7), 1172-1177.

665 He L, Kaifang Guan, Xu Li, Ying Ma & Zhou S (2019) MFG-E8 induced differences in
666 proteomic profiles in mouse C2C12 cells and its effect on PI3K/Akt and ERK
667 signal pathways. International Journal of Biological Macromolecules. 124,
668 681-688.

669 He L, Xu W, Ma Y & Zhou S (2017) Separation and Purification of Bovine Milk Fat
670 Globule Membrane Protein and Its Effect on Improvement of C2C12 Mouse
671 Skeletal Muscle Cell Proliferation. New Journal of Chemistry. 41(14),
672 6530-6539.

673 Janssen I & Ross R (2005) Linking age-related changes in skeletal muscle mass and
674 composition with metabolism and disease. Journal of Nutrition Health & Aging.
675 9(6), 408-419.

676 Jean F, Stine Klejs R, Inge Skovgaard K, Frank DP, Mackey AL & Kristian V (2014)
677 Whey protein supplementation accelerates satellite cell proliferation during
678 recovery from eccentric exercise. Amino Acids. 46(11), 2503-2516.

679 Jensen CB, Martin-Gronert MS, Storgaard H, Madsbad S & Ozanne SE (2008) Altered
680 PI3-Kinase/Akt Signalling in Skeletal Muscle of Young Men with Low Birth
681 Weight. Plos One. 3(11), e3738. <http://dx.doi.org/10.1371/journal.pone.0003738>.

682 Ji X, Li X, Ma Y & Li D (2017) Differences in proteomic profiles of milk fat globule
683 membrane in yak and cow milk. Food Chemistry. 221(15), 1822-1827.

684 Jianbo, Xi, Yaocheng, Sun, Meiting, Zhang, Zhenzhong, Fa, Yanya & Wan (2019) GLS1
685 promotes proliferation in hepatocellular carcinoma cells via
686 AKT/GSK3 β /CyclinD1 pathway. Experimental Cell Research. 381(1), 1-9.
687 <http://dx.doi.org/10.1016/j.yexcr.2019.04.005>.

688 Joe BBLBDQ (2019) Mitophagy regulates mitochondrial network signaling, oxidative
689 stress, and apoptosis during myoblast differentiation. Autophagy. 15(9),
690 1606-1619.

691 Li H, Guan K, Li X, Ma Y & Zhou S (2019) MFG-E8 induced differences in proteomic
692 profiles in mouse C2C12 cells and its effect on PI3K/Akt and ERK signal
693 pathways. *International Journal of Biological Macromolecules*. 124, 681-688.

694 Li H, Ma Y, Xu W, Chen H & Day L (2017) MFG-E8 protein promotes C2C12
695 myogenic differentiation by enhancing PI3K/Akt signaling. *New Journal of*
696 *Chemistry*. 41(20), 12061-12070.

697 Li H, Xu W, Ma Y, Zhou S & Xiao R (2018) Milk fat globule membrane protein
698 promotes C2C12 cell proliferation through the PI3K/Akt signaling pathway.
699 *International Journal of Biological Macromolecules*. 114, 1305-1314.

700 Liao C, Xin L, Jing L, Hua L, Yanshen Y, Jia L, Zihao G, Ke X, Chen Z & Jiankang L
701 (2014) D-galactose induces a mitochondrial complex I deficiency in mouse
702 skeletal muscle: potential benefits of nutrient combination in ameliorating
703 muscle impairment. *Journal of Medicinal Food*. 17(3), 357-364.

704 M; Nair K Sreekumaran; Kahn C Ronald; ONBTBGPCMKMNTSBPAKKPKLMPHDJ
705 (2019) FoxO Transcription Factors Are Critical Regulators of Diabetes-Related
706 Muscle Atrophy. *Diabetes*. 68(3), 556-570.

707 Manning BD & Toker A (2017) AKT/PKB Signaling: Navigating the Network. *Cell*.
708 169(3), 381-405.

709 Minegishi Y, Ota N, Soga S & Shimotoyodome A (2016) Effects of Nutritional
710 Supplementation with Milk Fat Globule Membrane on Physical and Muscle
711 Function in Healthy Adults Aged 60 and Over with Semiweekly Light Exercise:
712 A Randomized Double-Blind, Placebo-Controlled Pilot Trial. *Journal of*
713 *Nutritional Science & Vitaminology*. 62(6), 409-415.

714 Nguyen HT, Madec MN, Ong L, Kentish SE, Gras SL & Lopez C (2016) The dynamics
715 of the biological membrane surrounding the buffalo milk fat globule investigated
716 as a function of temperature. *Food Chemistry*. 204, 343-351.

717 Pandey P, Dixit A, Tanwar A, Sharma A & Mittal S (2014) A comparative study to
718 evaluate liquid dish washing soap as an alternative to xylene and alcohol in

719 deparaffinization and hematoxylin and eosin staining. *Journal of Laboratory*
720 Physicians. 6(2), 84-90.

721 Ponziani FR & Gasbarrini A (2018) Sarcopenia in patients with advanced liver disease.
722 *Current Protein & Peptide Science*. 19(7), 681-691.

723 Punga AR, Maj M, Lin S, Meinen S & Rüegg MA (2015) MuSK levels differ between
724 adult skeletal muscles and influence postsynaptic plasticity. *European Journal of*
725 Neuroscience. 33(5), 890-898.

726 Qi-chen Y, Bi-yuan Z, Min D, Rui C, Tian-ge L & Xue-ying M (2019) Dietary milk fat
727 globule membrane regulates JNK and PI3K/Akt pathway and ameliorates type 2
728 diabetes in mice induced by a high-fat diet and streptozotocin. *Journal of*
729 Functional Foods. 60, 103435-103444.

730 Ruiz JR, Larrarte E, Margareto J, Ares R & Labayen I (2012) Role of β 2-Adrenergic
731 Receptor Polymorphisms on Body Weight and Body Composition Response to
732 Energy Restriction in Obese Women: Preliminary Results. *Obesity*. 19(1),
733 212-215.

734 Rygiel K, Dodds R, Patel H, Syddall H, Westbury L, Granic A, Cooper C, Cliff J, Rocha
735 M & Turnbull D (2017) Association of mitochondrial respiratory chain
736 deficiency in older men with muscle mass and physical performance: findings
737 from the Hertfordshire Sarcopenia Study. *Lancet*. 389, 87.

738 Sakuma K, Aoi W & Yamaguchi A (2017) Molecular mechanism of sarcopenia and
739 cachexia: recent research advances. *Pflügers Archiv - European Journal of*
740 Physiology. 469(5-6), 1-19.

741 Sakuma K & Yamaguchi A (2018) Recent advances in pharmacological, hormonal, and
742 nutritional intervention for sarcopenia. *Pflügers Archiv: European Journal of*
743 Physiology. 470(3), 449-460.

744 Sun J, Zhang L, Zhang J, Ran R, Shao Y, Li J, Jia D, Zhang Y, Zhang M & Wang L
745 (2018) Protective effects of ginsenoside Rg1 on splenocytes and thymocytes in
746 an aging rat model induced by d-galactose. *International Immunopharmacology*.
747 58, 94-102.

748 Swiątecka D, Złotkowska D, Markiewicz LH, Szyc AM & Wróblewska B (2017)
749 Impact of whey proteins on the systemic and local intestinal level of mice with
750 diet induced obesity. *Food & Function*. 8(4), 1708-1717.

751 TF F, CP H, GA SL & C S (2003) PI3K/Akt and apoptosis: size matters. *Oncogene*.
752 22(56), 8983-8998.

753 Viana JU, Silva SL, Torres JL, Dias JM, Pereira LS & Dias RC (2013) Influence of
754 sarcopenia and functionality indicators on the frailty profile of
755 community-dwelling elderly subjects: a cross-sectional study. *Revista Brasileira*
756 *De Fisioterapia*. 17(4), 373-381.

757 Wang L, Wang Z, Yang K, Shu G, Wang S, Gao P, Zhu X, Xi Q, Zhang Y & Jiang Q
758 (2016) Epigallocatechin Gallate Reduces Slow-Twitch Muscle Fiber Formation
759 and Mitochondrial Biosynthesis in C2C12 Cells by Repressing AMPK Activity
760 and PGC-1 α Expression. *Journal of agricultural and food chemistry*. 64(34),
761 6517-6523.

762 Webster JR, Corson ID, Littlejohn RP, Martin SK & Suttie JM (2001) The roles of
763 photoperiod and nutrition in the seasonal increases in growth and insulin-like
764 growth factor-1 secretion in male red deer. *Animal Science*. 73(2), 305-311.

765 Wei LF, Zhang HM, Wang SS, Jing JJ, Zheng ZC & Gao JX (2016) Changes of MDA
766 and SOD in Brain Tissue after Secondary Brain Injury with Seawater Immersion
767 in Rats. *Turkish Neurosurgery*. 26(3), 384-388.

768 Yamane T, Morioka Y, Kitaura Y, Iwatsuki K & Oishi Y (2017) Branched-chain amino
769 acids regulate type I tropocollagen and type III tropocollagen syntheses via
770 modulation of mTOR in the skin. *Bioscience Biotechnology & Biochemistry*.
771 82(4), 611-615.

772 Yu M, Wang H, Xu Y, Yu D, Li D, Liu X & Du W (2015) Insulin-like growth factor-1
773 (IGF-1) promotes myoblast proliferation and skeletal muscle growth of
774 embryonic chickens via the PI3K/Akt signalling pathway. *Cell Biology*
775 *International*. 39(8), 910-922.

776 Yuan Z, Liling D, Chunmei W, Lianji Z & Geng Z (2018) Konjac glucomannan
777 improves hyperuricemia through regulating xanthine oxidase, adenosine
778 deaminase and urate transporters in rats. *Journal of Functional Foods*. 48,
779 566-575.

780 Zammit & S. P (2017) Function of the myogenic regulatory factors Myf5, MyoD,
781 Myogenin and MRF4 in skeletal muscle, satellite cells and regenerative
782 myogenesis. *Seminars in Cell & Developmental Biology*. 72, 19-32.

783 Zecic A & Braeckman BP (2020) DAF-16/FoxO in *Caenorhabditis elegans* and Its Role
784 in Metabolic Remodeling. *Cells*. 9(1), 1-15.
785 <http://dx.doi.org/10.3390/cells9010109>.

786 Zhang J, Lin W, Wu R, Liu Y, Zhu K, Ren J, Zhang S & Ling X (2018) Mechanisms of
787 the active components from Korean pine nut preventing and treating
788 d-galactose-induced aging rats. *Biomedicine & Pharmacotherapy*. 103, 680-690.

789 Zhou Y, Xu Q, Ying D, Zhu S, Song S & Sun N (2016) Supplementation of mussel
790 peptides reduces aging phenotype, lipid deposition and oxidative stress in
791 D-galactose-induce aging mice. *Journal of Nutrition Health & Aging*. 21(10),
792 1-7.

793
794
795

796 **Table**

797 **Table 1.** Primer sequence

798 **Table 2.** Animal grouping and feeding conditions

799 **Table 3.** The effects of D-gal on soleus and gastrocnemius coefficient of rat

800
801

Table 1. Primer sequence

Primer	Forward primer	Reverse primer
IGF-1	TGGTGGACGCTCTTCAGTTC	CTTCAGCGGAGCACAGTACA
Cyclin D1	CTGACACCAATCTCCTCAACGAC	GCGGCCAGGTTCCACTTGAGC

MyoD	TCAGGTGCTTTGAGAGATCGAC	CGAAAGGACAG-TTGGGAAGAGT
MyoG	AGAGAAGCACCTGCTCAAC	TGATCTCCTGGGTTGGGACC
GAPDH	ACCACAGTCCATGCCATCAC	TC-CACCACCCTGTTGCTGTA
MusK	AACAACATTCCCGTCCATAACG	GTGAGGAGAGCAAACACCG
Dok-7	TCTTTTCGGCCTGTCCACTC	TATCTGTGCGTAACGCGAGG

802

803

804

Table 2. Animal grouping and feeding conditions

Animal group	Number of rats	Basic feed	Amount	Feeding cycle	
Construction of rat model (6 week)	Normal	12	SPF animal feed	0.01 mol/L PBS	6 week
	Model (D-gal)	36	SPF animal feed	200 mk/kg D-gal	6 week
	Control	12	SPF animal feed	0.01 mol/L PBS	4 week
Nutritional intervention (4 week)	MFGM	12	SPF animal feed	16 mg MFGM	4 week
	MFG-E8	12	SPF animal feed	16 mg MFG-E8	4 week

805

806

807

Table 3. Effect of D-gal on soleus and gastrocnemius coefficient of rats

	Construction of rat model (6 week)	
	Normal	Model (D-gal)
Initial weight (g)	200±10.21 ^a	200±12.56 ^a
Final weight (g)	442.1±12.43 ^a	412.4±10.31 ^b
Soleus coefficient (%)	0.16±0.011 ^a	0.14±0.013 ^b
Gastrocnemius coefficient (%)	0.72±0.031 ^a	0.60±0.024 ^b

808

Note: values are means ± SEM of 10~12 rats. a-b means with different letters within a row are significantly ($p<0.05$).

809

810

Table 4. Effect of MFG-E8 on gastrocnemius and soleus coefficient of sarcopenic model rats

Nutritional intervention (4 week)

	Control	MFGM	MFG-E8
Initial weight (g)	412.4±10.31 ^b	412.4±10.31 ^b	412.4±10.31 ^b
Final weight (g)	455.67±10.34 ^a	464.00±12.46 ^{ab}	474.33±18.43 ^b
Soleus coefficient (%)	0.068±0.008 ^a	0.075±0.005 ^a	0.083±0.002 ^b
Gastrocnemius coefficient (%)	0.522±0.048 ^a	0.586±0.017 ^b	0.755±0.175 ^c

811 Notes: values are means ± SEM of 10~12 rats. a-b means with different letters within a row are
812 significantly ($p<0.05$).

813 **Figure Legend**

814 **Fig. 1** The work flow in this study.

815 **Fig. 2** Construction of sarcopenic model rats. (A) Effect of D-gal on body weight of rats;
816 (B) Effect of D-gal on tissue weights in rat; (C) Effect of D-gal on oxidation associated
817 biomarkers in blood; (D) Effect of D-gal on muscle fiber morphology. The results are
818 expressed as mean±SEM of 10~12 rats, the different letters (a-b) between control and
819 D-gal group across all represent significant differences ($p<0.05$).

820 **Fig. 3** Effect of MFG-E8 on improvement of muscle atrophy. (A) Effect of MFG-E8 on
821 tissues; (B) Effect of MFG-E8 on IGF-1; (C) Effect of MFG-E8 on SOD and MDA; (D)
822 Effect of MFG-E8 on GPT and GOT; (E) Effect of MFG-E8 on TG and NEFA. The
823 results are expressed as mean±SEM of 10~12 rats, the different letters between the three
824 groups of them across all represent significant differences ($p<0.05$).

825 **Fig. 4** Pathological section of rat liver and gastrocnemius. (A) Histological examination
826 of liver sections, black arrows indicate central veins, yellow arrows indicate lipid
827 droplets. blue arrows indicate hepatocytes. (B) Histological examination of
828 gastrocnemius sections.

829 **Fig. 5** Identification of myoblasts. (A) Morphology of myoblasts; (B) Myoblast
830 differentiation.

831 **Fig. 6** The effect of MFG-E8 on myoblasts activity was evaluated by *in vitro*. (A) Effect
832 of MFG-E8 on cell cycle; (B) Effect of MFG-E8 on mitochondria was observed by
833 TEM; (C) CLSM observed the effect of MFG-E8 on cell apoptosis.

834 **Fig. 7** Effect of MFG-E8 on the formation of neuromuscular junction. (A) Effects of

835 MFG-E8 on mRNA levels of MyoD, MyoG, cyclin D1, MusK, Dok-7 and IGF-1; (B)
836 Effect of MFG-E8 on protein levels of MusK. The results are expressed as mean±SEM
837 of 10~12 rats, the different letters (a-c) between the three groups of them across all
838 represent significant differences ($p<0.05$).

839 **Fig. 8** Effect of MFG-E8 on PI3K, p-PI3K, Akt, p-Akt, mTOR, p-mTOR, P70S6K,
840 p-P70S6K, 4E-BP and p-4E-BP expression in rat. The results are expressed as
841 mean±SEM of 10~12 rats, the different letters (a-c) between the three groups of them
842 across all represent significant differences ($p<0.05$).

843 **Fig. 9** The mechanism of MFG-E8 in gastrocnemius repair and regeneration. Based on
844 *in vivo* and *in vitro* results, we proposed that MFG-E8 in gastrocnemius repair and
845 regeneration might be described as follows: i) MFG-E8 promotes the regulatory and
846 catalytic subunit of PI3K and promote myoblast proliferation via
847 PI3K/Akt/mTOR/P70S6K and PI3K/Akt/mTOR/4E-BP signal pathway (Li et al. 2018);
848 ii) MFG-E8 can activate the PI3K/Akt pathway during myoblast differentiation process,
849 and regulate the expression of MyoD and MyoG (Li et al. 2017).

850

851

852

853

854

855

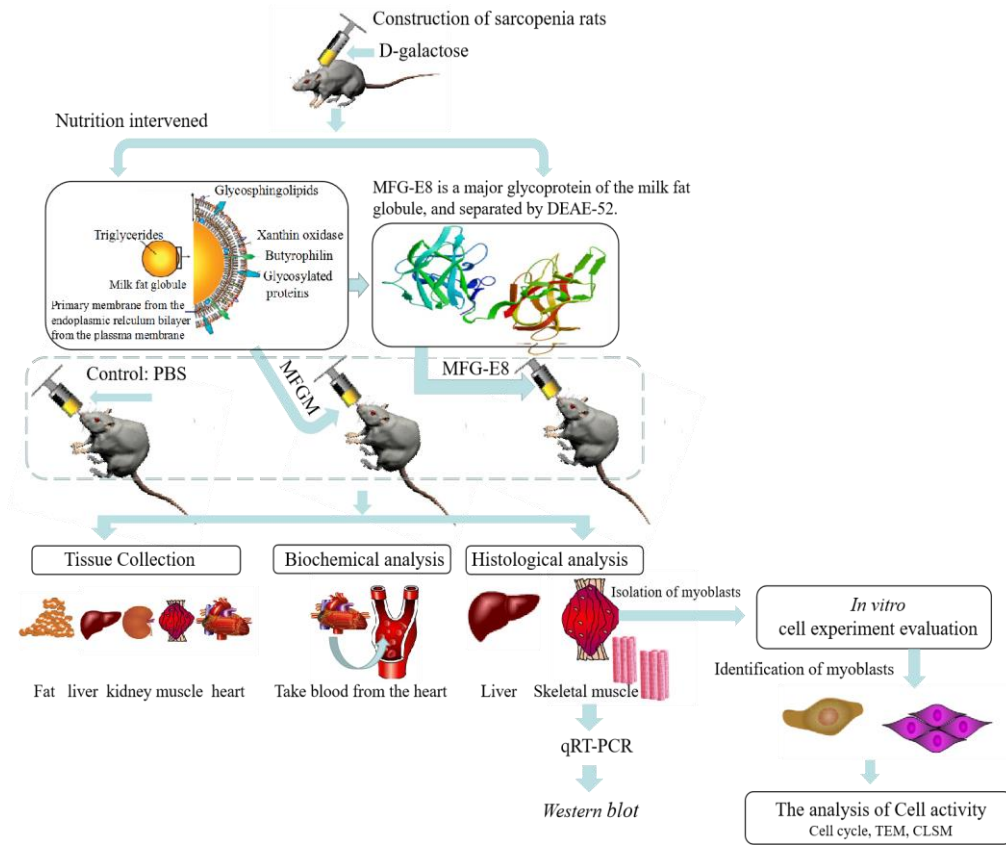
856

857

858

859

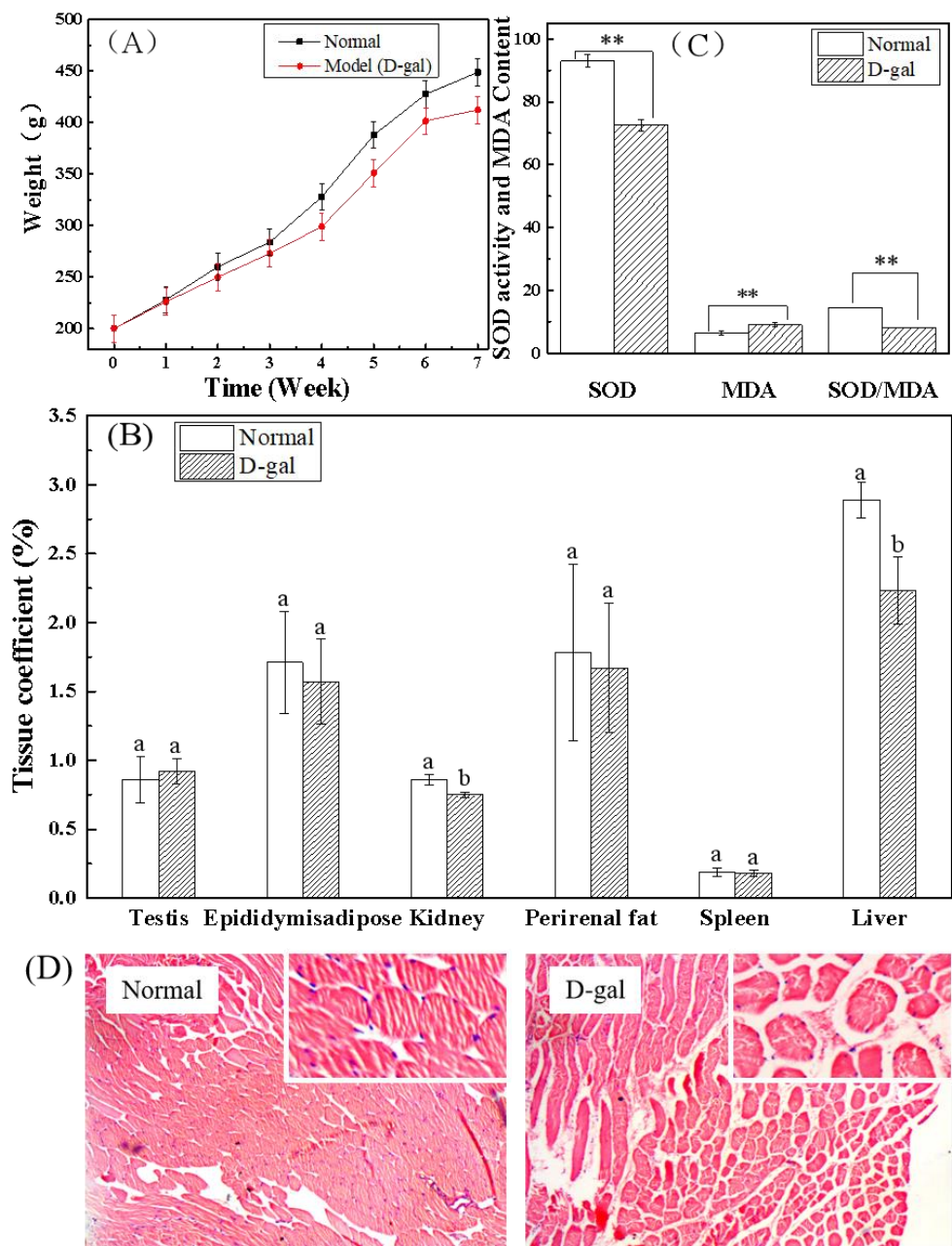
860



861

862

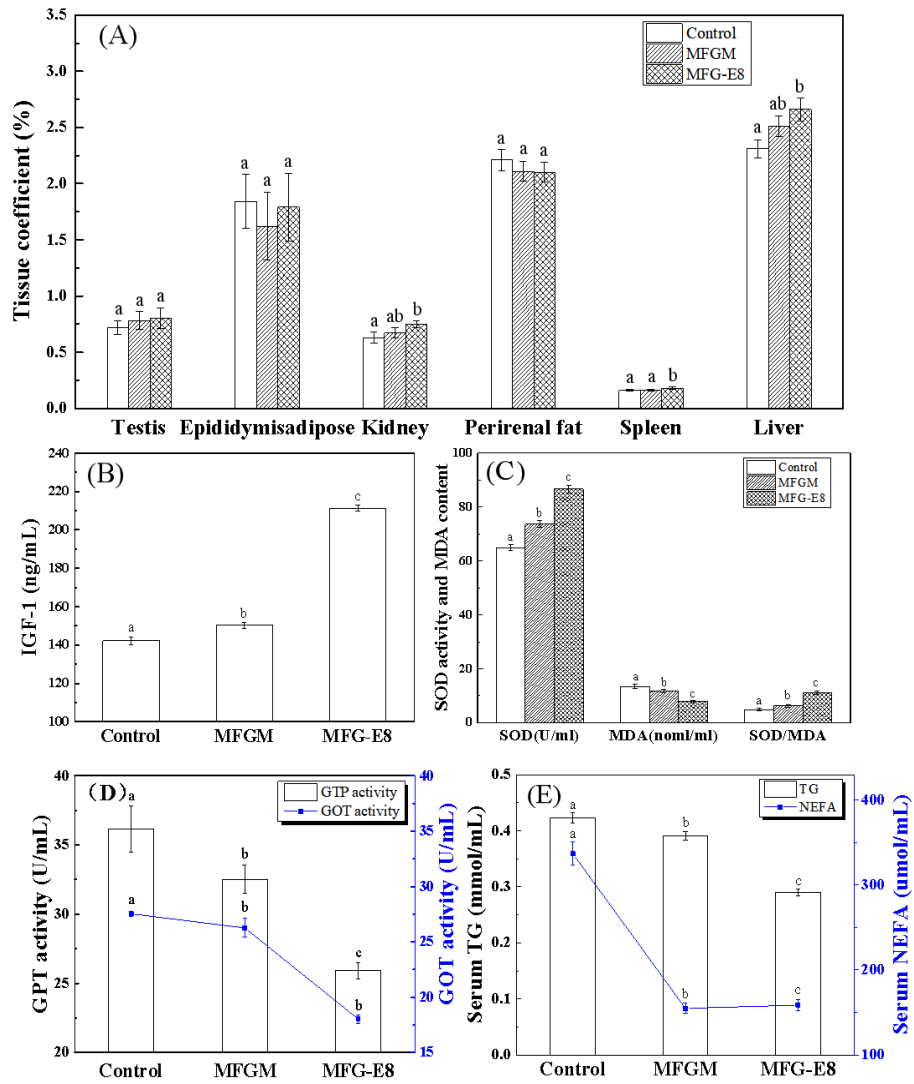
Fig. 1



863

864

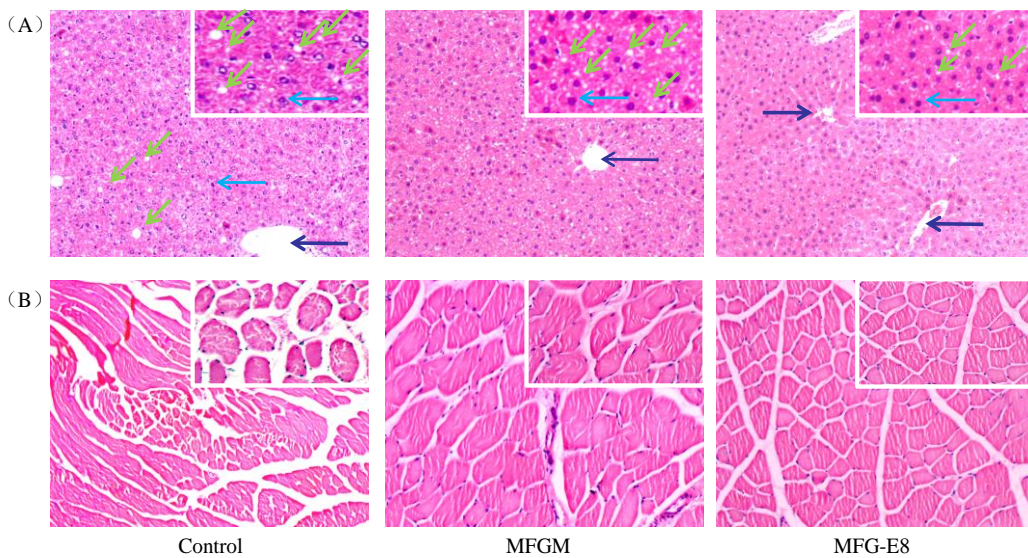
Fig. 2



865

866

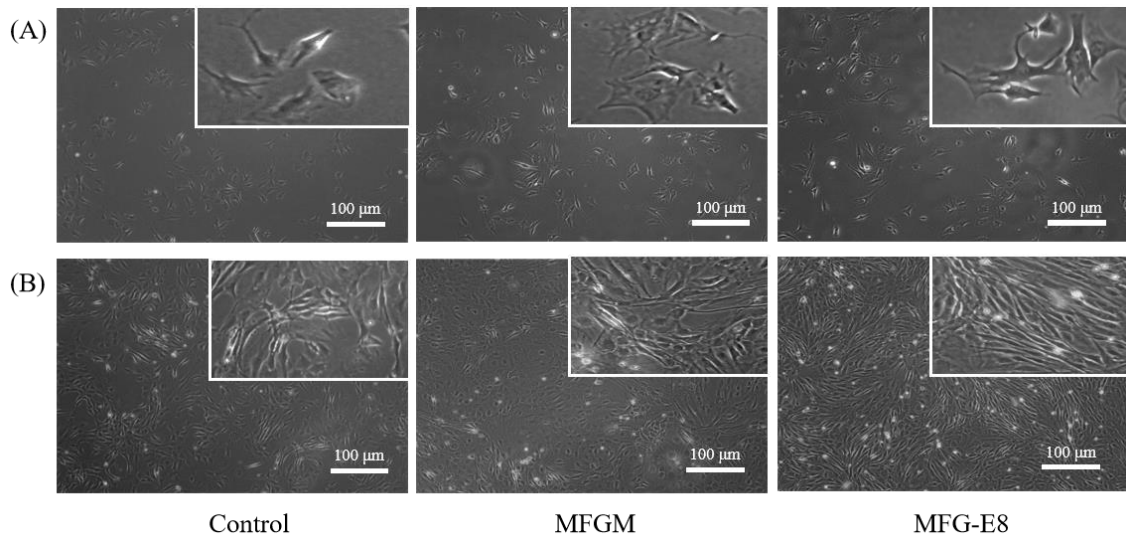
Fig. 3



867

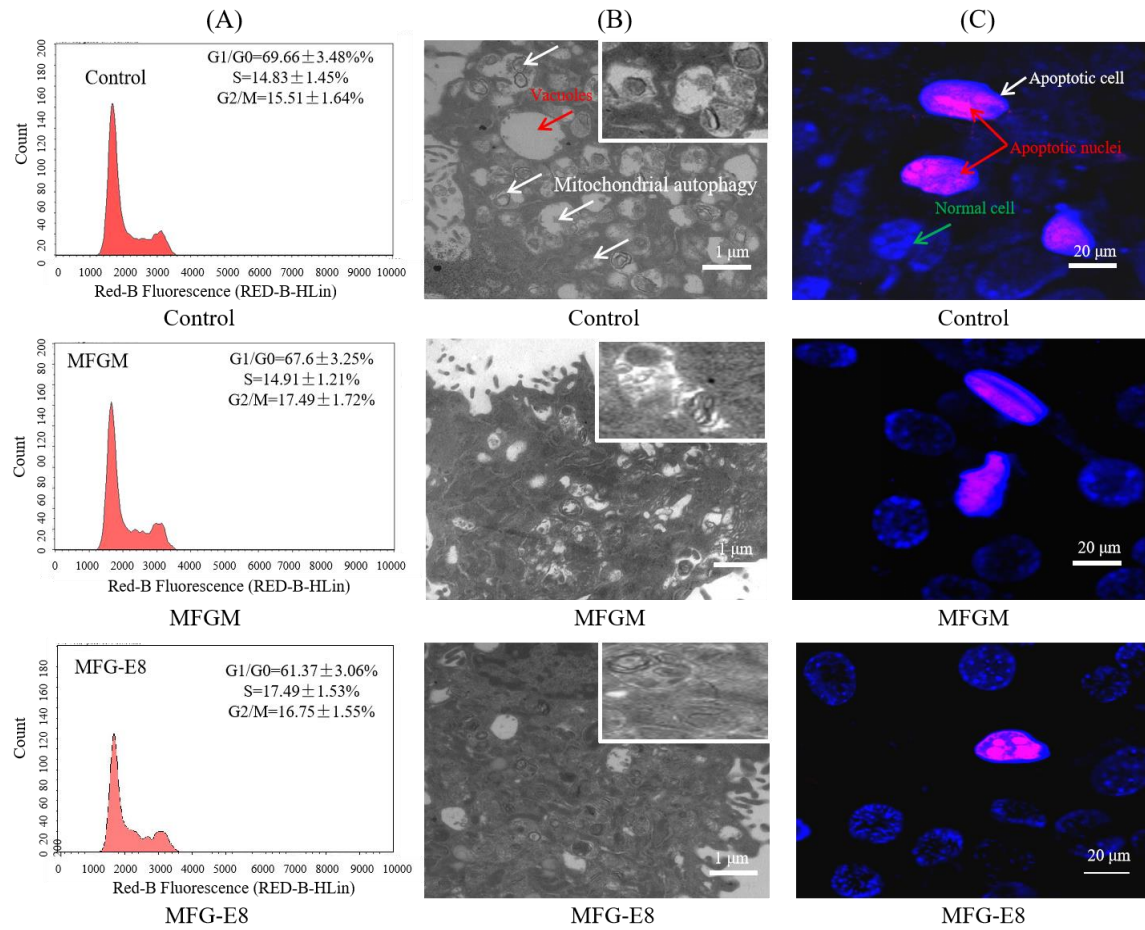
868

Fig. 4



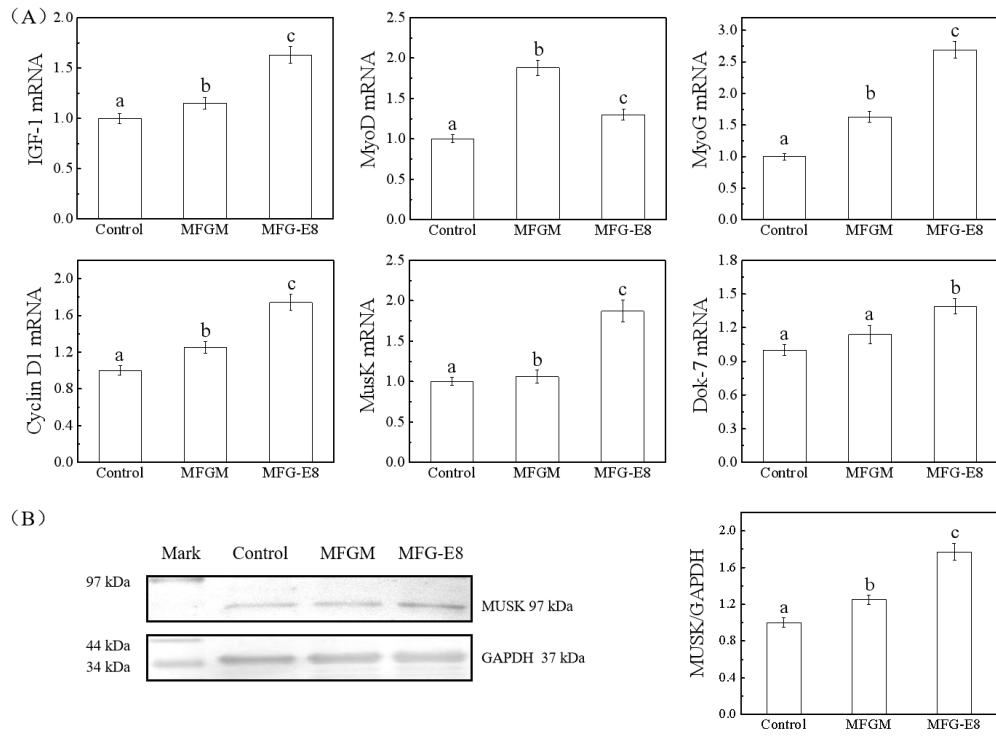
869
870
871

Fig. 5



872
873

Fig. 6

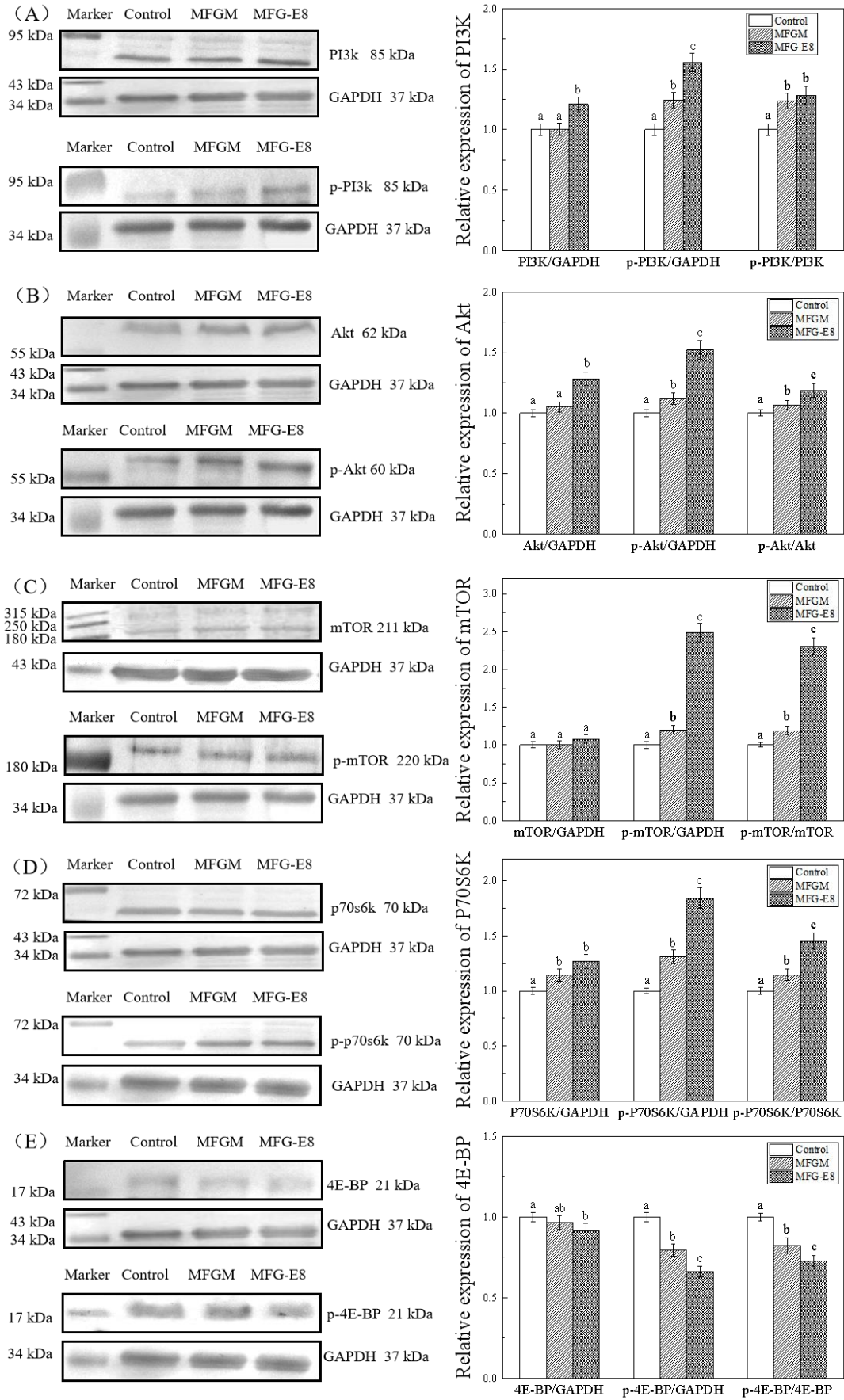


874

875

876

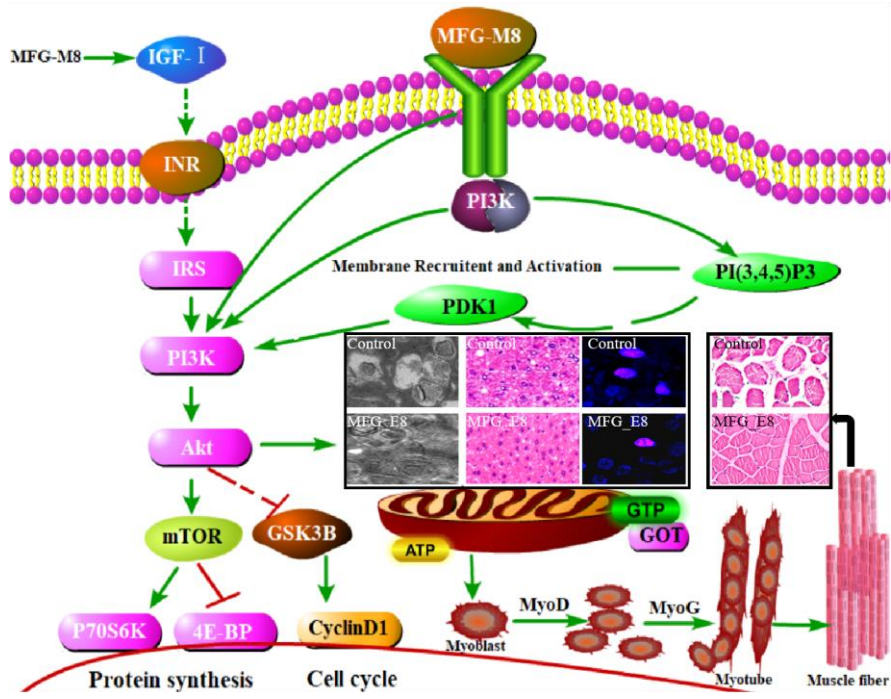
Fig. 7



877

878

Fig. 8



879

880

Fig. 9